Supporting Information for

The Timeless Relevance of Size-Match Selectivity in Macrocyclic Fe(III) Complexes

Sara Camorali,[a] Alessandro Nucera,[a,b] Marco Saccone,[a] Fabio Carniato,[a] Mauro Botta,[a] Francesco Blasi,[b] Zsolt Baranyai*[c] and Lorenzo Tei,*[a]

[a.] *Dipartimento di Scienze ed Innovazione Tecnologica, Università del Piemonte ` Orientale, Viale T. Michel 11, 15121 Alessandria, Italy.*
[b.] *Bracco Research Centre, Bracco Imaging S.p.A., Via Ribes 5, 10010 Colleretto Giacosa, Italy.*
[c.] *CRB Trieste, Bracco Imaging SpA, AREA Science Park, 34149 Basovizza (TS), Italy*

Table of Contents:

I. Equilibrium studies

The protonation constants, defined by Eq. (S1), were determined by pH-potentiometry and ^{1}H-NMR spectroscopy.

$$K_i^H = \frac{[H_iL]}{[H_{i-1}L][H^+]} \qquad (S1)$$

where i=1, 2…5. The protonation sequence of DETA, UNTA and DOTRA has been determined by ^{1}H-NMR spectroscopy, recording the chemical shift variations of the non-labile protons as a function of pH. The ^{1}H-NMR titration curves (Figures S1, S2 and S3) display sharp changes at certain pH values, which are related to the protonation/deprotonation of the ligand. Since the protonation/deprotonation is fast on the NMR time scale, the chemical shifts of the observed signals represent a weighted average of the shifts of the different species involved in a specific protonation step (Eq. (S2))[1]:

$$\delta_{obs} = \sum x_i \delta^{H_iL} \qquad (S2)$$

where, δ_{obs} is the observed chemical shift of a given ^{1}H NMR signal, x_i and δ^{H_iL} are the molar fraction and the chemical shift of the involved species, respectively. The observed chemical shifts (δ_{obs}) have been fitted to the Eq. (S2), respectively (the molar fractions x_i and the concentration of the different protonated species have been expressed by the protonation constants K_i^H, Eq. (1)). The fittings of the experimental data points are shown in Figures S1, S2 and S3.

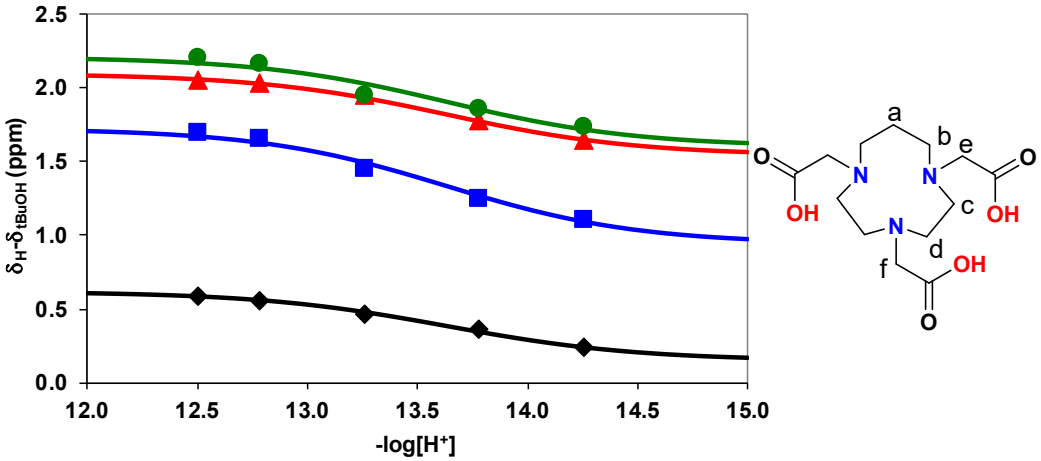

Figure S1. The chemical shifts of the different protons of DETA ligand as a function of -log[H$^+$]. The solid lines and the symbols represent the the calculated and the experimental chemical shift values, respectively. (a (✹), b, c and d (■), e (▲) and f (●) [DETA]=0.01 M, I=[$NaNO_3$]+[NaOH]=0.15 M, [NaOH]≤0.15 M, 25°C).

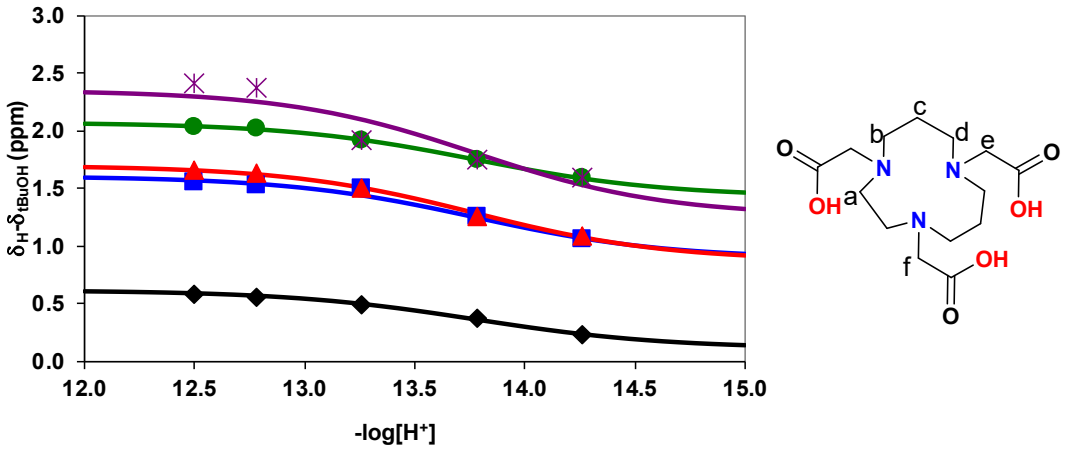

Figure S2. The chemical shifts of the different protons of UNTA ligand as a function of -log[H^+]. The solid lines and the symbols represent the the calculated and the experimental chemical shift values, respectively. (a, b and d (■, ▲), c (✹), e (ᛉ) and f (●), [UNTA]=0.01 M, I=[$NaNO_3$]+[NaOH]=0.15 M, [NaOH]≤0.15 M, 25°C).

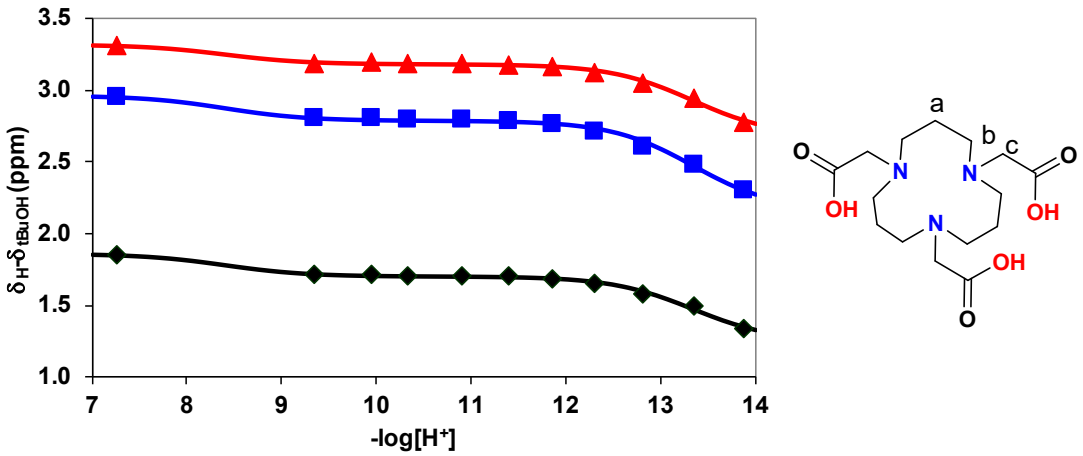

Figure S3. The chemical shifts of the different protons of DOTRA ligand as a function of -log[H^+]. The solid lines and the symbols represent the the calculated and the experimental chemical shift values, respectively. (a (✹), b (■) and c (▲), [DOTRA]=0.01 M, I=[$NaNO_3$]+[NaOH]=0.15 M, [NaOH]≤0.15 M, 25°C)

The ^{1}H-NMR spectra of DETA, UNTA and DOTRA are very complicated and rich in signals, particularly at pH>10. Based on the previous studies,[2] the first two protonations result in deshielding of all methylen protons with different extents indicating that all nitrogen atoms of symmetric NOTA and DOTRA are equally protonated, whereas there are preferential protonations of the nitrogen atoms in the asymmetric DETA and UNTA ligands. Detailed ^{1}H NMR studies revealed that the first protonation of DETA and UNTA take place predominantly by the formation sixmembered rings with the involvement of the nitrogen atoms of the propylene groups, whereas the second protonation occur on all nitrogen atoms partially. Further protonation of NOTA, DETA, UNTA and DOTRA take place at the carboxylate groups of the acetic arms attached to the ring nitrogen atoms.[2]

The protonation constants of Fe(III) complexes with NOTA, DETA, UNTA and DOTRA have been determined by pH-potentiometric titrations of the complexes in the pH range 1.7 – 12.0 (Figures S4 - S7).

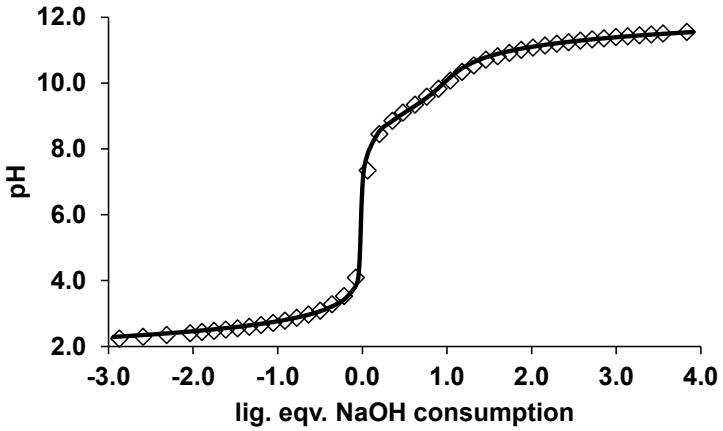

Figure S4. pH potentiometric titration profile of Fe^{3+} – NOTA – H^+ system. Open symbols and the solid line represent the measured and the calculated pH values, respectively. ([Fe^{3+}]=[H_3NOTA]=2.0 mM, 0.15 M $NaNO_3$, 25°C)

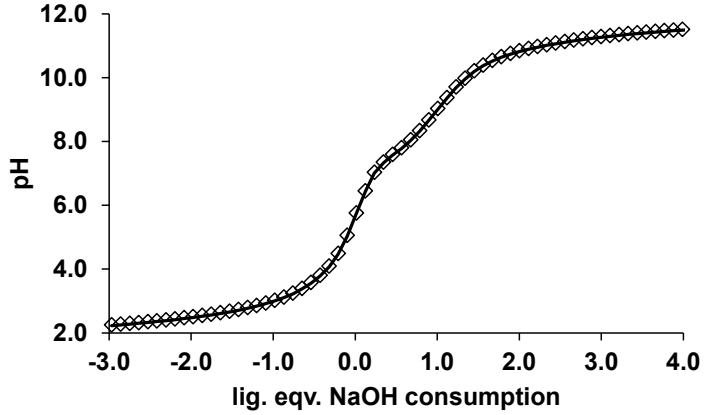

Figure S5. pH potentiometric titration profile of Fe^{3+} – DETA – H^+ system. Open symbols and the solid line represent the measured and the calculated pH values, respectively. ([Fe^{3+}]=[H_3DETA]=2.0 mM, 0.15 M $NaNO_3$, 25°C)

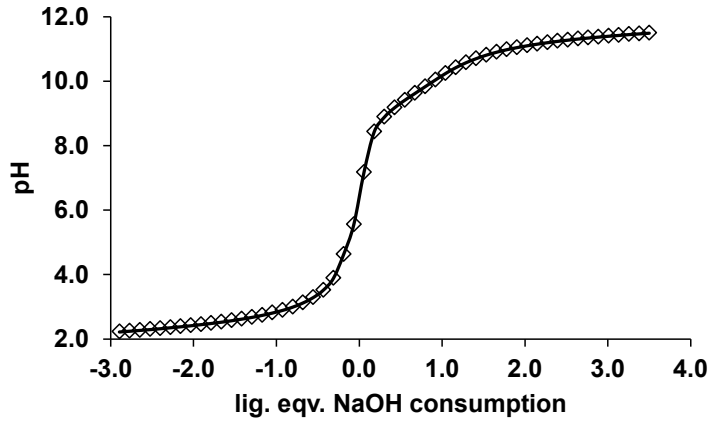

Figure S6. pH potentiometric titration profile of Fe^{3+} – UNTA – H^+ system. Open symbols and the solid line represent the measured and the calculated pH values, respectively. ([Fe^{3+}]=[H_3UNTA]=2.0 mM, 0.15 M $NaNO_3$, 25°C)

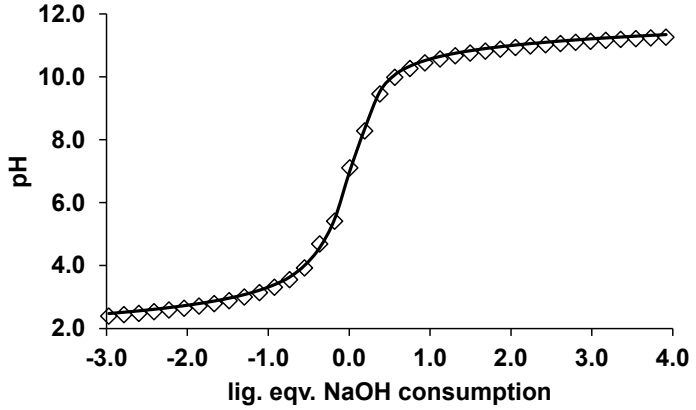

Figure S7. pH potentiometric titration profile of Fe^{3+} – DOTRA – H^+ system. Open symbols and the solid line represent the measured and the calculated pH values, respectively. ([Fe^{3+}]=[H_3DOTRA]=2.0 mM, 0.15 M $NaNO_3$, 25°C)

At pH>6.0 the titrations curves indicate the base consumption process which can be interpreted by the hydrolysis of the Fe(III) ion with the coordination of OH^- ion (Eq. (S3)) and by the dimerization of the FeL (Eq. (S4)) and $FeLH_{-1}$ species (Eq. (S5)) via the formation of μ–oxo dimers.

$$FeLH_{-1} + H^+ \rightleftharpoons FeL \qquad (S3)$$

$$K_{FeLH_{-1}} = \frac{[FeL]}{[FeLH_{-1}][H^+]}$$

$$2FeL \rightleftharpoons [(FeL)_2(\mu\text{-}O)] + H^+ \qquad (S4)$$

$$K_D = \frac{[(FeL)_2(\mu - O)][H^+]}{[FeL]^2}$$

$$2FeLH_{-1} \rightleftharpoons [(FeL)_2(\mu\text{-}O)] \qquad (S5)$$

$$K_d = \frac{[(FeL)_2(\mu - O)]}{[FeLH_{-1}]^2}$$

According to the method proposed by Gustafson and Martell,[3] the protonation and dimerization constant of FeL and $FeLH_{-1}$ species were calculated from the pH potentiometric titration data ($[FeL]_{tot}$, $[NaOH]_{tot}$, pH, pA and pK_w) obtained for Fe(III) complexes with NOTA, DETA, UNTA and DOTRA by plotting the $[H^+](T_{OH} + [H^+] - [OH^-])/[FeL]$ as a function of $2[FeL]/[H^+]$, where $[FeL] = T_{FeL} - T_{OH} - [H^+] + [OH^-]$, T_{FeL} and T_{OH} are the total concentration of FeL complex and NaOH added beyond the formation of the FeL species. The slope of the straight line yields K_D and its intercept provides K_{FeLH-1} if the binuclear deprotonated species is the only polynuclear chelate present in measurable concentration. Moreover, the K_d value can be expressed by $K_d = K_D/K_{FeLH-1}^2$. $[H^+](T_{OH} + [H^+] - [OH^-])/[FeL]$ as a function of $2[FeL]/[H^+]$ for Fe(III) complexes with NOTA, DETA, UNTA and DOTRA are shown in Figures S8-S11. The $[H^+](T_{OH} + [H^+] - [OH^-])/[FeL]$ values as a function of $2[FeL]/[H^+]$ for Fe(III) complexes with NOTA, DETA, UNTA and DOTRA yield a straight line with negative slopes, which confirms the absence or the negligible concentration of the polynuclear chelate in our experimental condition.

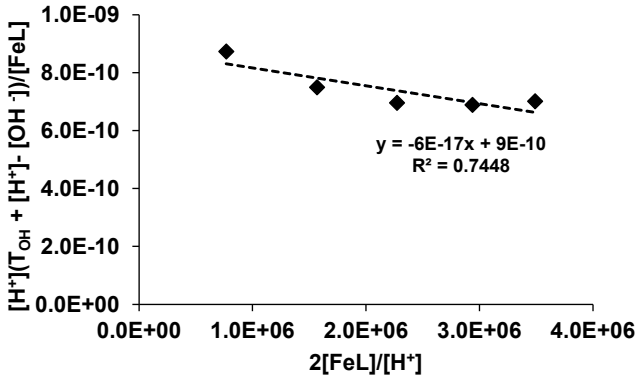

Figure S8. $[H^+](T_{OH} + [H^+] - [OH^-])/[FeL]$ values as a function of $2[FeL]/[H^+]$ for [Fe(NOTA)] ([Fe(NOTA)]=2.0 mM, 0.15 M $NaNO_3$, 25°C)

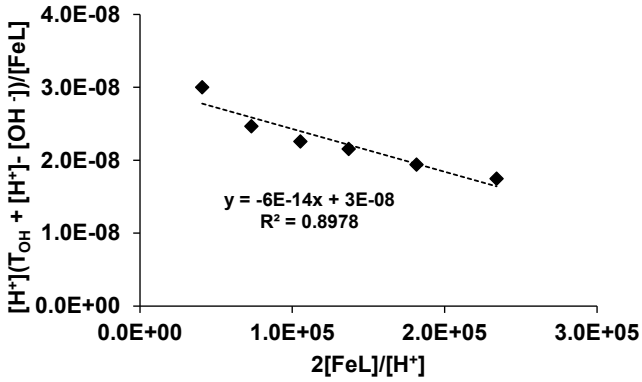

Figure S9. $[H^+](T_{OH} + [H^+]- [OH^-])/[FeL]$ values as a function of $2[FeL]/[H^+]$ for [Fe(DETA)] ([Fe(DETA)]=2.0 mM, 0.15 M $NaNO_3$, 25°C)

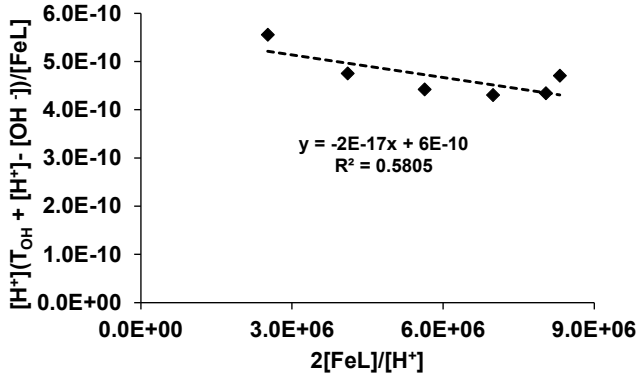

Figure S10. $[H^+](T_{OH} + [H^+]- [OH^-])/[FeL]$ values as a function of $2[FeL]/[H^+]$ for [Fe(UNTA)] ([Fe(UNTA)]=2.0 mM, 0.15 M $NaNO_3$, 25°C)

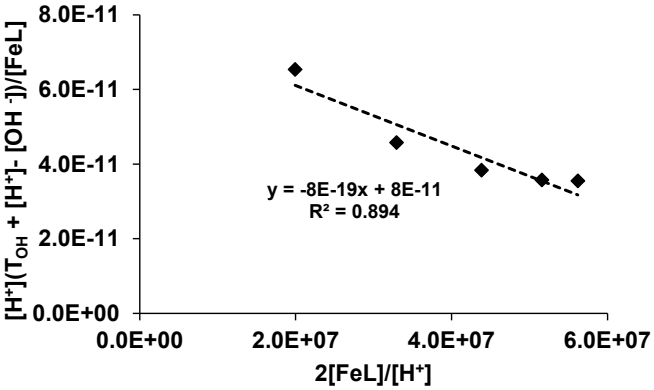

Figure S11. $[H^+](T_{OH} + [H^+]- [OH^-])/[FeL]$ values as a function of $2[FeL]/[H^+]$ for [Fe(DOTRA)] ([Fe(DOTRA)]=2.0 mM, 0.15 M $NaNO_3$, 25°C)

II. Cyclic voltammetry

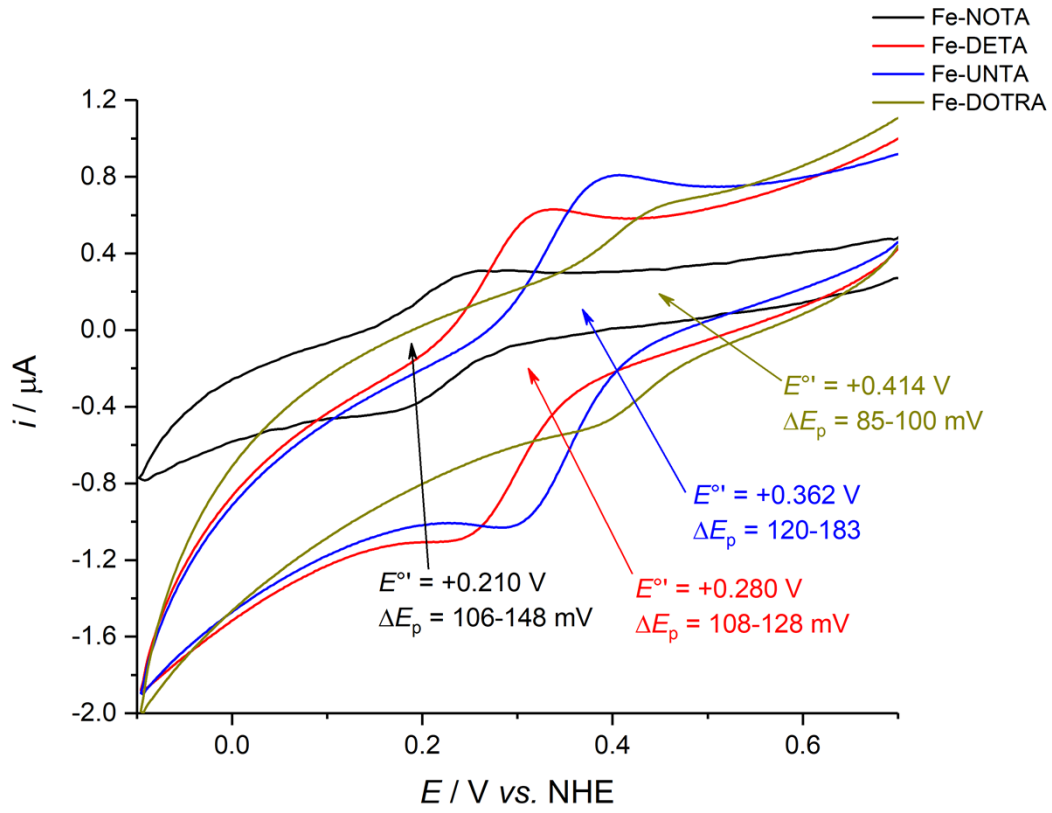

Figure S12. Cyclic voltammograms recorded for [Fe(NOTA)] (black), [Fe(DETA)] (red), [Fe(UNTA)] (blue) and [Fe(DOTRA)] (green) with indicated the $E_{1/2}$ vs. NHE (V) and the ΔE_p. Experimental conditions: 0.3 mM [FeL] in an aqueous solution containing 0.15 M KNO_3 at pH = 7.0 and 25°C; working electrode = glassy carbon; scan rate = 0.2 V s^{-1}.

III. Kinetic studies

The kinetic inertness of [Fe(NOTA)], [Fe(DETA)], [Fe(UNTA)] and [Fe(DOTRA)] complexes was determined by following the transchelation reactions with HBED ligand (Eq. (S6) with spectrophotometry on the absorption band of the resulting $[Fe(HBED)]^-$ in the pH range 7.5 – 12.5 ($\log K_{Fe(HBED)}$=39.68, 0.1 M KNO_3, 25°C).[4] The exchanging HBED ligand was applied in 10 and 20 fold excess to establish pseudo-first-order kinetic conditions ([FeL]=0.2 mM, 0.15 M $NaNO_3$, 25°C).

$$FeL + HBED \rightleftharpoons Fe(HBED) + L \qquad (L=NOTA, DETA, UNTA, DOTRA) \qquad (S6)$$

In the presence of excess of the exchanging HBED ligand the transchelation is pseudo-first-order process and the rate of reactions can be expressed with the Eq. (S7), where k_d is a pseudo-first-order rate constant and $[GdL]_t$ is the total concentration of the complex.

$$-\frac{d[FeL]_t}{dt} = k_d[FeL]_t \qquad (S7)$$

The rates of the transmetallation reactions were studied at different concentrations of the HBED ligand in the pH range 7.4 – 12.5. The obtained pseudo-first order rate constants k_d are presented in Figure S13 as a function of [OH$^-$].

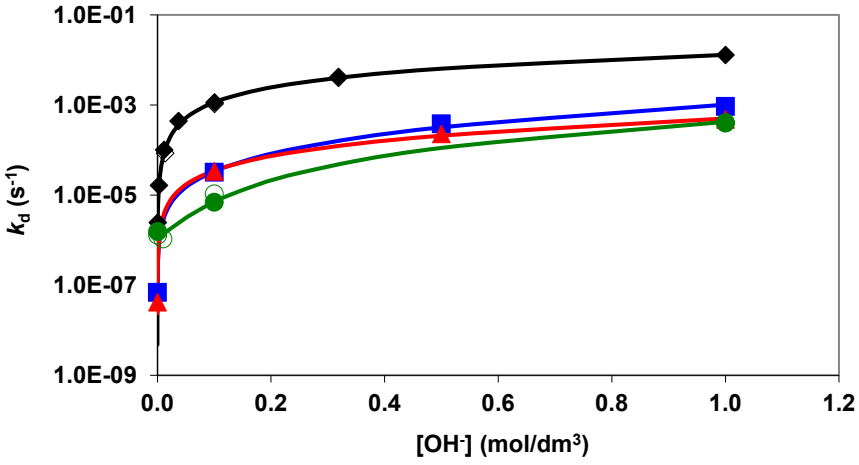

Figure S13. Pseudo-first order rate constants (k_d) characterizing the transchelation reaction of **[Fe(NOTA)]**, **[Fe(DETA)]**, **[Fe(UNTA)]** and **[Fe(DOTRA)]** complexes with HBED ligand ([FeL]=0.2 mM, [HBED]=2.0 (⊕, ○, □, ∞) and 4.0 mM (✱, ∞), I=[Na$^+$]+[H$^+$]=0.15 M, [H$^+$]≤0.15 M, 25°C).

By taking into account the species distribution of Fe^{3+} - NOTA, Fe^{3+} - DETA, Fe^{3+} - UNTA and Fe^{3+} - DOTRA systems, the dependence of the k_d values on [OH$^-$] can be interpreted as spontaneous dissociation (k_0, Eq. (S8)) and OH^--ion assisted dissociation (k_{OH}, Eq. (S9) and k_{OH}^2, Eq. (S10)) of the $FeLH_{-1}$ species dominates in the investigated pH ranges.

$$FeLH_{-1} \xrightarrow{k_0} Fe^{3+} + L + OH^- \qquad (S8)$$

$$FeLH_{-1} + OH^- \xrightarrow{k_{OH}} Fe^{3+} + L + 2OH^- \qquad (S9)$$

$$FeLH_{-1} + 2OH^- \xrightarrow{k_{OH}^2} Fe^{3+} + L + 3OH^- \qquad (S10)$$

By taking into account all possible pathways and Eq. (S7), the rate of the dissociation of Fe(III) complexes with NOTA, DETA, UNTA and DOTRA can be expressed by Eq. (S11).

$$-\frac{d[FeL]_t}{dt} = k_d[FeL]_t = k_0[FeLH_{-1}] + k_{OH}[FeLH_{-1}][OH^-] + k_{OH}^2[FeLH_{-1}][OH^-]^2 \qquad (S11)$$

Considering the total concentration of the Fe(III) complexes ($[FeL]_t=[FeL]+[FeLH_{-1}]$) and the protonation constant of $FeLH_{-1}$ (K_{FeLH-1}), the k_d pseudo-first-order rate can be expressed by Eq. (S12).

$$k_d = \frac{k_0 + k_{OH}(K_W/[H^+]) + k_{OH}^2(K_W/[H^+])^2}{1 + K_{FeLH_{-1}}[H^+]} \qquad (S12)$$

wherein k_0, k_{OH} and k_{OH}^2 are the rate constants characterizing the spontaneous and OH^- assisted dissociation of $FeLH_{-1}$ species, K_w is the stoichiometric water ionic product, whereas K_{FeLH-1} is the protonation constant of the $FeLH_{-1}$ species. k_0, k_{OH} and k_{OH}^2 rate constants were calculated by fitting of the k_d vs. $[OH^-]$ data (Figure S13) to Eq. (S12).

IV. Computational details

All calculations were performed at the DFT level using the GAUSSIAN 16 (Rev. C.01) quantum-chemistry package,[5] and the B3LYP functional.[6] For geometry optimizations and vibrational frequency analysis (no imaginary frequencies were found), the pcseg-2 basis set of Jensen of triple-ζ-quality and optimized for DFT calculations,[7] was used for all atoms. Electron densities were used as the starting point for further analysis including IRI,[8] QTAIM,[9] and employing the AIMAll (version 11.05.16),[10] and Multiwfn (version 3.8) software.[11] For both the IRI and QTAIM analysis a grid with an ultra-high resolution of 5 pm was employed. The VMD (version 1.9.4) software was used for visualization purposes.[12]

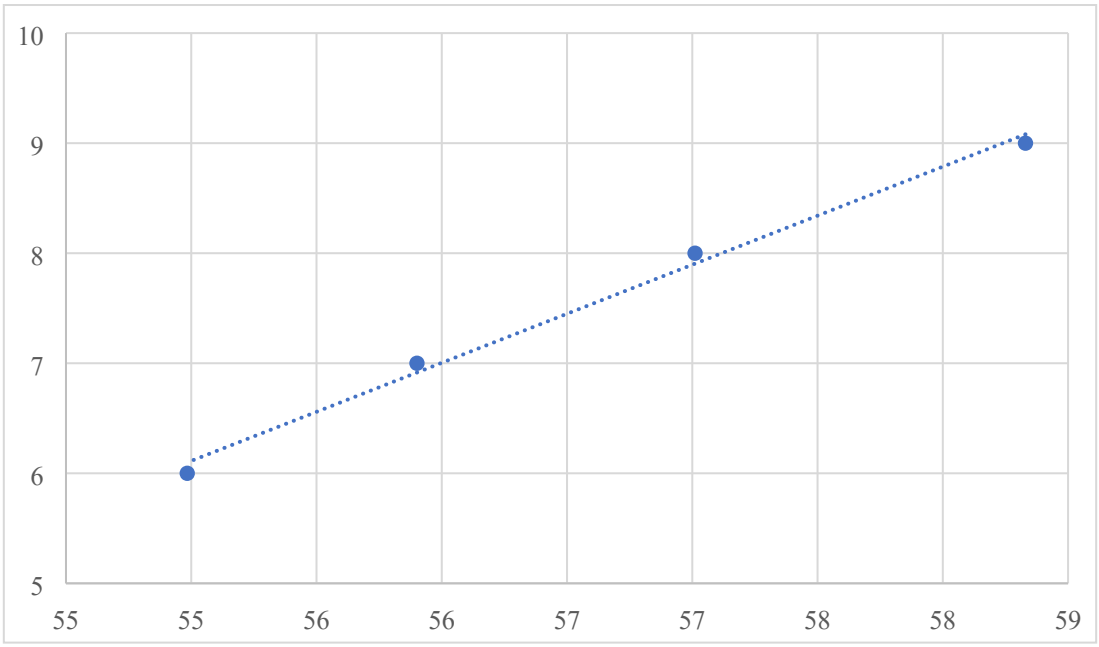

Figure S14. The number of CH_2 groups vs the iron atomic volume shows a linear correlation.

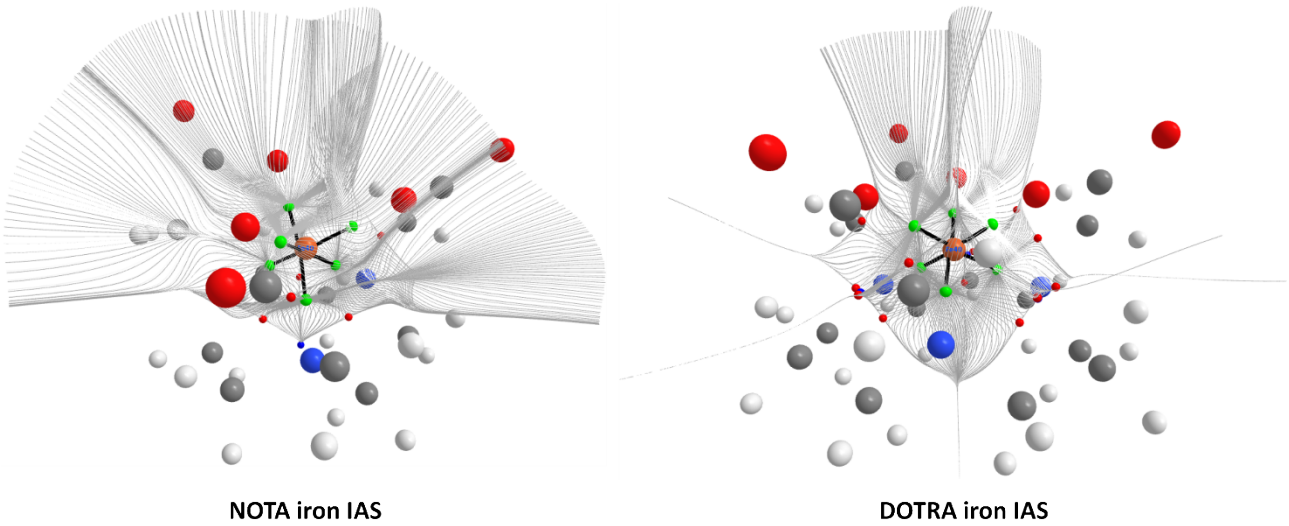

Figure S15. The interatomic surfaces of the iron atoms in the [Fe(NOTA)] and [Fe(DOTRA)] complexes.

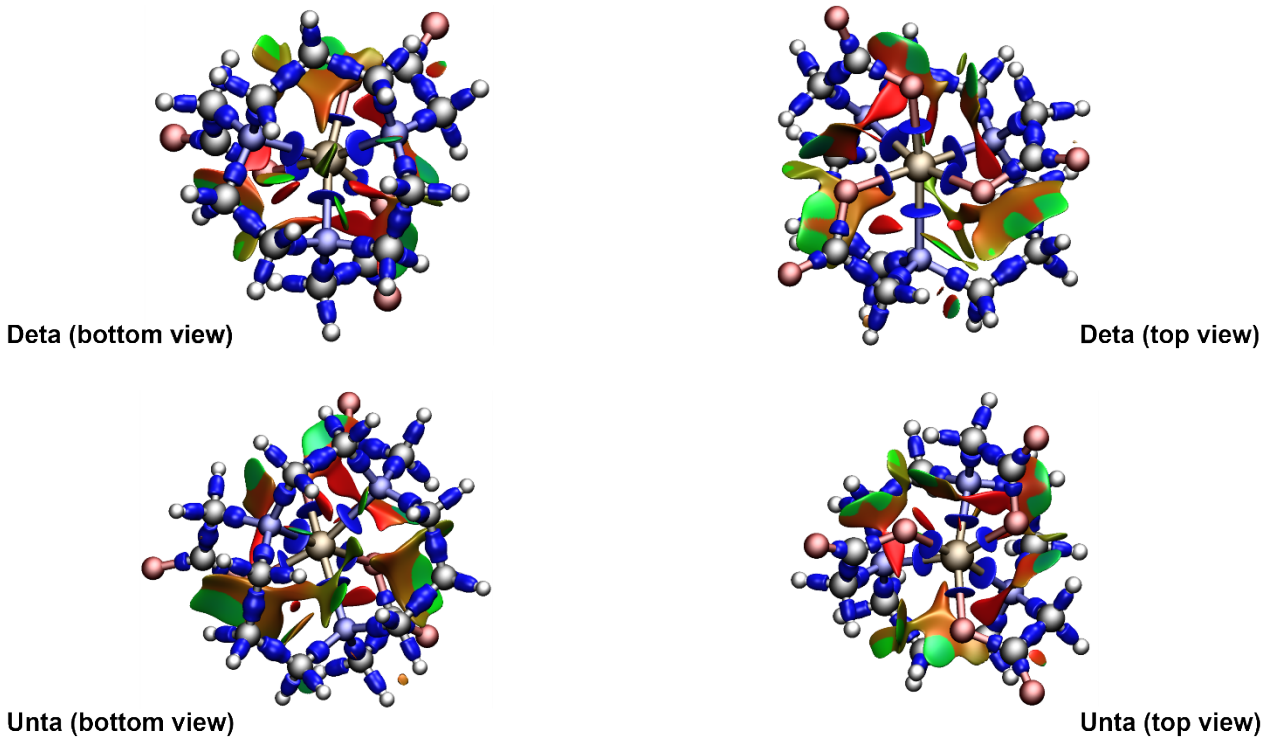

Figure S16. Top and bottom views of the IRI isosurfaces of the [Fe(DETA)] and [Fe(UNTA)] complexes.

V. DFT Optimized Coordinates

[Fe(NOTA)]

Symbol	NA	NB	NC	Bond	Angle	Dihedral	X	Y	Z
O							1.0634372	1.2535764	1.2954091
O	1			2.2467660			1.0017714	3.4242272	1.8719765
C	2	1		1.2086217	27.8667168		0.6539018	2.4898802	1.1887862
C	1	3	2	3.0381880	146.4705189	-116.9319968	2.5216324	-1.0551577	-0.0365068
C	4	1	3	2.5275807	77.0986213	-24.6625508	1.7147908	0.3124134	-2.0030826
C	4	1	3	2.4428486	102.3119191	-79.2557848	0.8175489	-1.9486422	-1.5415963
H	4	1	3	1.0882375	55.8018553	68.7098986	3.0032319	-0.1373160	0.2949891
H	5	4	1	1.0890522	130.1866009	-135.7688072	1.2471705	-0.0038703	-2.9343884
H	5	4	1	1.0908444	81.0110839	120.0195300	2.7880749	0.3581048	-2.1925949
H	6	4	1	1.0936728	102.6016971	146.2815734	1.4090764	-2.2907684	-2.3955079
H	6	4	1	1.0855537	78.1217742	-108.0361098	0.8667899	-2.7183916	-0.7777324
O	1	3	2	2.8137317	93.5908781	127.8606618	-1.5479300	0.2124180	1.4130385
O	4	1	3	2.3815208	59.0390085	-144.3055297	0.6448395	-1.4437655	1.3770963
C	3	2	1	1.5511039	119.9218367	-177.4468468	-0.3341989	2.7154732	0.0146106
C	13	4	1	1.3037504	36.6875124	-124.7655853	1.8973142	-1.7554627	1.1929309
C	5	4	1	1.5282662	112.6185638	12.1635221	1.2016013	1.6911520	-1.5891814

C	6	4	1	1.5261553	140.6027817	-1.4393408	-0.6359411	-1.7191142	-1.9463599
C	16	5	4	2.4770372	100.0035096	-108.4360755	-1.2288201	1.3698072	-1.9434450
C	12	1	3	2.3889692	120.5254779	132.3991886	-2.1717680	-1.6550144	0.0600062
C	18	16	5	1.5280189	129.4997621	47.0596600	-2.1298868	0.2145194	-1.5095896
C	12	1	3	1.3063072	154.4233575	153.9459383	-2.4552033	-0.7141526	1.2556838
H	14	3	2	1.0885385	108.7032042	-85.2828706	-1.3507773	2.6803639	0.4022336
O	15	13	4	1.2097668	126.4916667	-178.0329272	2.5504640	-2.5304988	1.8534234
H	16	5	4	1.0935108	110.4952043	161.9740509	1.1638179	2.3607632	-2.4528706
H	16	5	4	1.0848098	109.6205097	43.4879943	1.8782974	2.1287956	-0.8629840
H	17	6	4	1.0892382	110.6926982	101.8943730	-0.6918368	-1.1895320	-2.8965484
H	17	6	4	1.0909480	110.1456285	-140.3848681	-1.1412149	-2.6751543	-2.0907670
H	18	16	5	1.0891544	74.6714268	-57.1881471	-0.7665725	1.1539698	-2.9057333
H	18	16	5	1.0907113	116.4448291	-158.4528640	-1.8237366	2.2739641	-2.0784482
H	19	12	1	1.0888008	106.9302731	66.7241613	-1.6053908	-2.5117628	0.4215116
H	20	18	16	1.0934138	110.6340774	-129.8811121	-2.7249447	-0.1475187	-2.3524349
H	20	18	16	1.0854385	109.5050379	111.7932815	-2.8204476	0.5602221	-0.7468366
O	21	12	1	1.2092136	126.3682390	149.0945333	-3.4508711	-0.8638367	1.9253389
H	4	1	3	1.0911453	165.2988771	60.7711848	3.2579878	-1.7034060	-0.5141604
H	14	3	2	1.0913210	110.1607725	34.6178061	-0.1547567	3.6882413	-0.4463713
H	19	12	1	1.0911170	134.5809209	-151.0239437	-3.1054586	-1.9978636	-0.3885611
N	14	3	2	1.4854759	107.4402455	157.0018836	-0.1463679	1.5982736	-0.9462344
N	17	6	4	1.4883827	110.1761621	-17.8689881	-1.3333805	-0.9035456	-0.9149972
N	4	1	3	1.4862284	74.6140708	-57.5544820	1.4092431	-0.7068944	-0.9585576
Fe	12	1	3	1.9109575	42.8111370	121.4264226	-0.0052034	0.0063519	0.3043050

[Fe(DETA)]

Symbol	NA	NB	NC	Bond	Angle	Dihedral	X	Y	Z
Fe							-0.0756671	-0.0560544	-0.2787500
O	1			1.9228267			-1.4818738	0.8175882	-1.2568062
O	2	1		2.2517528	141.5803078		-2.1089110	2.8433278	-2.0141660
C	3	2	1	1.2144138	27.9176973	-11.9880702	-1.4087300	2.1219773	-1.3328432
C	1	2	4	2.7514939	74.8771976	134.8861880	-2.4000970	-1.2443914	0.5905020
C	5	1	2	2.5297729	66.2001834	-106.5689193	-1.3633206	0.3272821	2.2800843
C	5	1	2	2.4372398	65.6122771	-173.3820147	-0.4031174	-1.9297939	1.8080543
H	5	1	2	1.0941954	91.7163851	-21.4445395	-2.9980988	-0.3869273	0.2673724
H	6	5	1	1.0965845	134.5751987	-84.3636380	-0.5791152	0.2312626	3.0405444
H	6	5	1	1.0997082	83.8682890	167.9487019	-2.3264269	0.2156424	2.7990457
H	7	5	1	1.1009305	104.6704527	151.6830494	-0.7664406	-2.1946705	2.8129844
H	7	5	1	1.0909117	76.1323935	-103.7614083	-0.6141097	-2.7769013	1.1538528
O	1	2	4	1.9029419	93.8045784	-70.9361678	1.2397861	0.2950028	-1.6082347
O	1	13	2	1.9470566	96.4960493	87.2037544	-0.7257704	-1.7229171	-1.0468409
C	4	3	2	1.5372884	120.8568547	-178.4053853	-0.3272190	2.7125043	-0.4136765
C	14	1	13	1.3121507	113.2645050	-157.5449023	-1.9424536	-2.0303836	-0.6635842
C	6	5	1	1.5240548	106.0257799	58.2821226	-1.2791610	1.6858851	1.5946224

C	7	5	1	1.5253991	140.4159989	1.1388301	1.0978477	-1.6612280	1.8507027
C	17	6	5	2.4660821	103.2494173	-116.2976358	1.1473376	2.1095611	1.4756094
C	13	1	2	2.4021625	76.4425609	-153.9893309	2.0627712	-1.6755684	-0.5082668
C	20	13	1	2.4427916	77.9574043	-78.2009381	2.6759118	0.0837104	1.0716787
C	13	1	2	1.3229678	111.5391224	-144.4538527	2.1030622	-0.7020499	-1.7125612
H	15	4	3	1.0953676	108.5338967	-87.6649410	0.5969201	2.8248479	-0.9908905
O	16	14	1	1.2129747	126.4766542	166.2038445	-2.6644524	-2.8693034	-1.1598091
H	17	6	5	1.1006392	110.8365055	156.0269955	-1.2520718	2.4979648	2.3370504
H	17	6	5	1.0931348	109.7537141	37.7224660	-2.1657624	1.8424561	0.9746489
H	18	7	5	1.0945775	109.4125312	107.2557096	1.3368979	-1.0724430	2.7419306
H	18	7	5	1.0998667	109.7656706	-136.1807606	1.6431125	-2.6114645	1.9478818
H	19	17	6	1.0982570	78.2706185	-42.7632775	1.0400830	1.7100768	2.4929968
H	19	17	6	1.1004797	101.9438270	-147.4870241	1.1922307	3.2049571	1.5712539
H	20	13	1	1.0940904	106.2800501	66.0447550	1.3469792	-2.4725601	-0.7307074
H	21	20	13	1.0968476	124.5273591	158.9475466	2.8869777	-0.0817573	2.1352323
H	21	20	13	1.0958251	72.9326680	-102.8191793	3.5876424	-0.1957734	0.5318002
O	22	13	1	1.2110700	125.5465996	166.4463896	2.8933506	-0.8573805	-2.6169987
H	5	1	13	1.0987062	154.4422338	122.4365233	-2.9983877	-1.8835918	1.2542990
H	15	4	3	1.0990741	110.7228203	32.0510258	-0.6352081	3.6964787	-0.0330181
H	20	13	1	1.0981855	134.8477245	-151.4318658	3.0579911	-2.1034825	-0.3281604
C	19	17	6	1.5219840	141.7292553	64.5180762	2.4239518	1.5752626	0.8421928
H	38	19	17	1.0946656	110.2926816	72.7281602	2.4422321	1.8059092	-0.2277421
H	38	19	17	1.0996940	108.1675597	-170.9895991	3.2771317	2.1028526	1.2928143
N	6	5	1	1.4866313	32.0595453	-43.4594675	-1.1668045	-0.7535602	1.2784686
N	19	17	6	1.4900849	34.5545131	107.3603582	-0.0759141	1.7549375	0.7021429
N	18	7	5	1.4955369	112.7154868	-11.8532775	1.5794375	-0.8846076	0.6668266

[Fe(UNTA)]

Symbol	NA	NB	NC	Bond	Angle	Dihedral	X	Y	Z
Fe							0.0531442	0.1172954	-0.3129260
O	1			1.9256531			0.6812047	1.7727796	-1.0699280
O	2	1		2.2525187	138.6101280		2.6387057	2.8133335	-1.4690240
C	3	2	1	1.2130504	28.2377203	-23.5789415	1.9590274	2.0099773	-0.8655777
C	1	2	4	2.7164188	74.6027470	147.4257643	-2.0544809	1.8244379	-0.1628857
C	5	1	2	2.5209386	68.4644606	-94.5348620	-0.7246800	1.8055013	1.9787031
C	6	5	1	2.4181730	59.8955357	-81.5883640	-2.3616421	0.0775106	1.5521311
H	5	1	2	1.0941537	90.7540706	-12.1146773	-1.4050674	2.6705544	-0.4068557
H	6	5	1	1.0946903	130.4648869	-100.2584873	-0.9135017	1.2935466	2.9277002
H	6	5	1	1.0984246	80.2364208	156.4160715	-1.1951654	2.7947021	2.0603239
H	7	6	5	1.0957724	80.1655665	169.8689453	-1.8704682	-0.3441311	2.4362598
H	7	6	5	1.1015155	93.0134068	-83.7621001	-3.1957862	0.6959525	1.9196493
O	1	2	4	1.8993431	88.0656126	-52.8867232	1.4652996	-0.7627016	-1.2288552
O	1	13	2	1.9168546	102.0303467	91.1165594	-1.3740269	0.0172265	-1.5886614
C	4	3	2	1.5428021	120.9672407	-176.3816720	2.5419372	1.2039809	0.3137545
C	14	1	13	1.3111721	112.5518772	-152.7556658	-2.2355094	0.9969070	-1.4573356
C	6	5	1	1.5221925	113.3890206	48.8504097	0.7738073	1.9609741	1.7609099

C	7	6	5	2.5897521	126.6113893	90.9254608	-1.9381811	-2.1984689	0.3913495
C	17	6	5	2.4772858	106.0057715	-106.2947255	1.7591552	-0.2747360	2.1703424
C	13	1	14	2.3547168	81.8764528	-66.7452735	0.0430002	-2.6183344	-0.9488860
C	18	7	6	2.4470240	88.2527283	36.1748120	0.2517571	-2.2620238	1.4813302
C	13	1	14	1.3105897	118.5346917	-68.3491079	1.3648421	-2.0516741	-1.4435725
H	15	4	3	1.0920835	109.1901504	-82.7683554	3.0858109	0.3406514	-0.0754880
O	16	14	1	1.2147945	125.8956957	170.9614062	-3.1394426	1.2582752	-2.2256565
H	17	6	5	1.1007561	110.0884487	166.2532445	1.2726344	2.1910483	2.7147973
H	17	6	5	1.0899221	109.6025587	48.8113526	0.9609190	2.8012972	1.0924965
H	18	7	6	1.0993054	106.4767999	108.6556726	-2.0069096	-2.9659206	1.1754200
H	18	7	6	1.0917186	135.4763856	-115.4589140	-2.2707026	-2.6744937	-0.5331392
H	19	17	6	1.0987692	77.1184281	-46.6215373	1.0831612	-0.1444168	3.0266968
H	19	17	6	1.1005825	104.1713238	-150.7651455	2.7745782	-0.0588349	2.5358349
H	20	13	1	1.0951051	101.9178146	80.8283018	-0.6720690	-2.4806246	-1.7667901
H	21	18	7	1.0971386	80.3911891	44.9702143	-0.3665489	-1.9462853	2.3308713
H	21	18	7	1.1014989	93.3158970	151.0742288	0.2780000	-3.3629003	1.5074482
O	22	13	1	1.2146272	125.5009799	-177.9688925	2.2041785	-2.7444221	-1.9829555
H	5	1	13	1.0986374	156.3069077	146.8363662	-3.0258629	2.1947538	0.1924836
H	15	4	3	1.0993508	110.3038523	37.8272529	3.2211967	1.8328208	0.9068304
H	20	13	1	1.0986184	138.1541192	-141.3753381	0.1304163	-3.6894293	-0.7206833
C	19	17	6	1.5292226	141.7034663	56.9849929	1.6738143	-1.7279599	1.7019633
H	38	19	17	1.0944896	111.3046534	86.7132240	2.3220325	-1.9061055	0.8382593
H	38	19	17	1.0999235	106.1770180	-159.0206750	2.0949246	-2.3372516	2.5151431
N	6	5	1	1.4990197	32.9320578	-46.5271620	-1.3770975	1.0002204	0.8956823
N	19	17	6	1.4883301	34.1792736	106.4278257	1.3909503	0.7395792	1.1452979
N	20	13	1	1.4986051	84.3387834	-25.7163873	-0.4765288	-1.8544987	0.2311402
C	7	6	5	1.5181593	151.1495074	57.7064941	-2.9113493	-1.0521775	0.6998198
H	44	7	6	1.0924300	110.9349270	-71.4378279	-3.3515429	-0.6665703	-0.2226442
H	44	7	6	1.0994131	106.2640655	174.4829804	-3.7494051	-1.4845654	1.2649856

[Fe(DOTRA)]

Symbol	NA	NB	NC	Bond	Angle	Dihedral	X	Y	Z
O							-0.5563815	1.4685598	1.3410116
O	1			2.2448192			-2.3955568	2.4482075	2.1758395
C	2	1		1.2150846	28.4146947		-1.8495810	1.6635796	1.4257062
C	1	3	2	2.7820121	156.9071453	-88.1690184	2.0411249	1.8879393	0.4373120
C	4	1	3	2.4525327	76.9327443	-30.3564727	0.6724401	2.5143391	-1.4989840
C	5	4	1	2.4226462	60.4506639	-118.4354831	2.2397036	0.6766304	-1.6879970
H	4	1	3	1.0932724	52.8557730	60.9836743	1.3997802	2.6038004	0.9583346
H	5	4	1	1.0968388	130.7518316	-139.3323256	0.8153524	2.3215795	-2.5692527
H	5	4	1	1.0985220	75.9193017	121.1804680	1.2451570	3.4236424	-1.2711385
H	6	5	4	1.0977881	81.1585059	170.4386281	1.7084714	0.5438768	-2.6394735
H	6	5	4	1.1014664	91.1478892	-82.8556361	3.0688823	1.3748072	-1.8835481
O	1	3	2	2.7198196	89.3152317	134.5866215	-0.9941955	-1.2157905	1.3400709

O	4	1	3	2.3753411	63.0952369	-156.9010296	1.5497933	-0.2534451	1.3402581
C	3	2	1	1.5283967	121.1985625	-178.0698592	-2.6556419	0.8224846	0.4363521
C	13	4	1	1.3105509	36.2041225	-126.4177542	2.3659886	0.7683522	1.4256937
C	14	3	2	2.4542664	100.4369217	119.1230763	-1.7049562	1.6020408	-1.6877742
C	6	5	4	2.5533085	129.8080784	98.0379596	1.8403239	-1.8382599	-1.5003615
C	16	14	3	2.4223368	60.3805118	148.9575980	-2.5120500	-0.6742442	-1.5011151
C	12	1	3	2.3753699	120.8218274	157.4276335	0.6151608	-2.7111077	0.4365329
C	17	6	5	2.4223030	109.0593424	15.5735736	-0.5342877	-2.2782341	-1.6879628
C	12	1	3	1.3106117	149.1175315	-168.9827753	-0.5167227	-2.4333537	1.4252923
H	14	3	2	1.0933013	107.2138657	-87.8925735	-2.9542023	-0.0914822	0.9567694
O	15	13	4	1.2151188	125.4078741	-178.1879516	3.3188267	0.8475259	2.1755902
H	16	14	3	1.0977959	140.4448278	134.0323499	-1.3238438	1.2091284	-2.6393670
H	16	14	3	1.1014692	84.3671390	-116.4876238	-2.7241440	1.9710189	-1.8835955
H	17	6	5	1.0968402	89.1839798	87.1773186	1.6011796	-1.8642655	-2.5704980
H	17	6	5	1.0985433	142.7930556	-156.4529492	2.3414935	-2.7892749	-1.2740941
H	18	16	14	1.0968321	72.9301102	163.6822200	-2.4143231	-0.4540204	-2.5711579
H	18	16	14	1.0985450	107.7992177	61.6203480	-3.5863243	-0.6321822	-1.2753575
H	19	12	1	1.0932900	106.7098908	55.5841025	1.5557237	-2.5129279	0.9574447
H	20	17	6	1.0978032	81.1270178	57.1732542	-0.3836980	-1.7527878	-2.6400136
H	20	17	6	1.1014665	91.1868904	163.8656909	-0.3444181	-3.3456117	-1.8825979
O	21	12	1	1.2151171	125.4046019	128.2627147	-0.9239358	-3.2983212	2.1753045
H	4	1	3	1.0990234	161.4936929	41.6292804	2.9634940	2.3898858	0.1130632
H	14	3	2	1.0990160	110.3082765	31.2810222	-3.5518967	1.3696833	0.1121034
H	19	12	1	1.0990273	134.2375408	-163.2569454	0.5893843	-3.7609078	0.1123164
N	14	3	2	1.5012495	111.2096078	154.0879685	-1.8227887	0.4335503	-0.7505918
N	19	12	1	1.5010735	83.1702796	-51.3673513	0.5361053	-1.7954827	-0.7503128
N	4	1	3	1.5012501	74.6419701	-66.8311453	1.2871003	1.3625632	-0.7497764
Fe	12	1	3	1.9082890	44.5537859	129.6179452	-0.0002078	0.0002710	0.2562121
C	18	16	14	1.5242172	140.3998155	-99.2050358	-1.9932906	-2.0893122	-1.2737180
H	41	18	16	1.0914255	112.1779519	104.8506740	-2.2002601	-2.4466088	-0.2634148
H	41	18	16	1.1003910	105.6064312	-140.4626982	-2.5833632	-2.7322211	-1.9440483
C	17	6	5	1.5243007	33.2800826	-148.0105230	2.8060312	-0.6809161	-1.2735197
H	44	17	6	1.1004009	105.5934022	-115.6210972	3.6576172	-0.8704618	-1.9441581
H	44	17	6	1.0914264	112.1956228	129.6966199	3.2194947	-0.6808565	-0.2634408
C	5	4	1	1.5242448	118.0019969	16.0626735	-0.8127894	2.7714002	-1.2724111
H	47	5	4	1.0914321	112.1717582	28.4777064	-1.0195241	3.1287258	-0.2620631
H	47	5	4	1.1003933	105.6052948	143.1531806	-1.0746747	3.6040782	-1.9424327

VI. Relaxometry

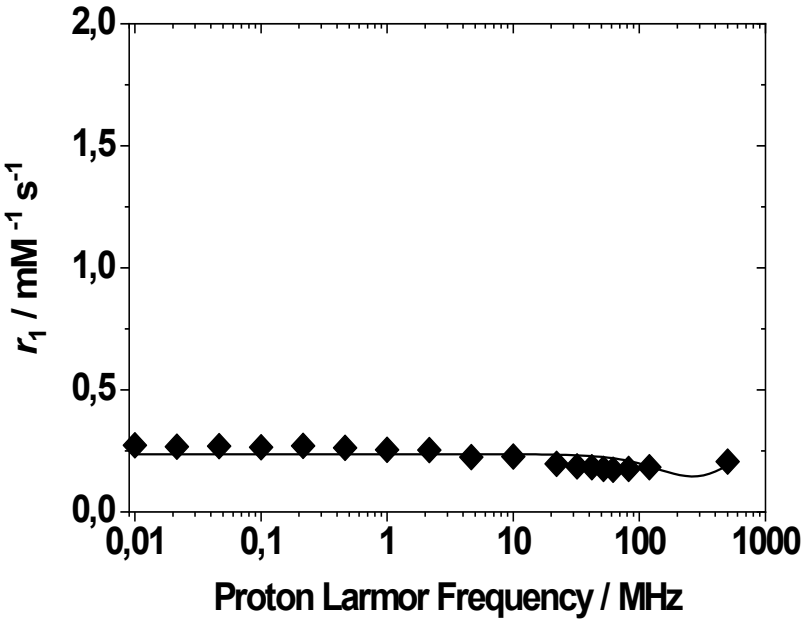

Figure S17. ^{1}H NMRD profile of [Fe(DETA)] in aqueous solution at pH = 10 and 25°C; [Fe^{3+}] = 3.0 mM.

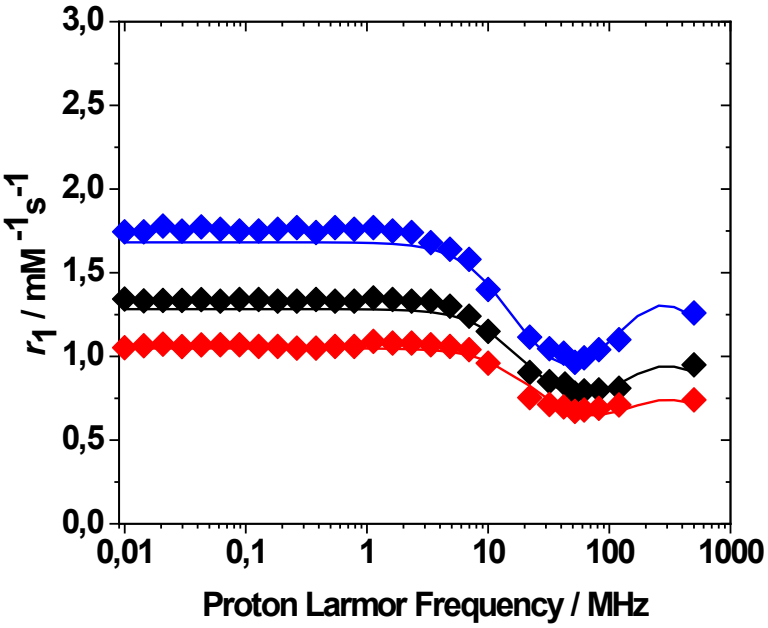

Figure S18. ^{1}H NMRD profiles of [Fe(NOTA)] in aqueous solution at pH = 7.5 and at different temperatures (10°C, blue; 25°C, black; 37°C, red) [Fe^{3+}] = 1.5 mM.

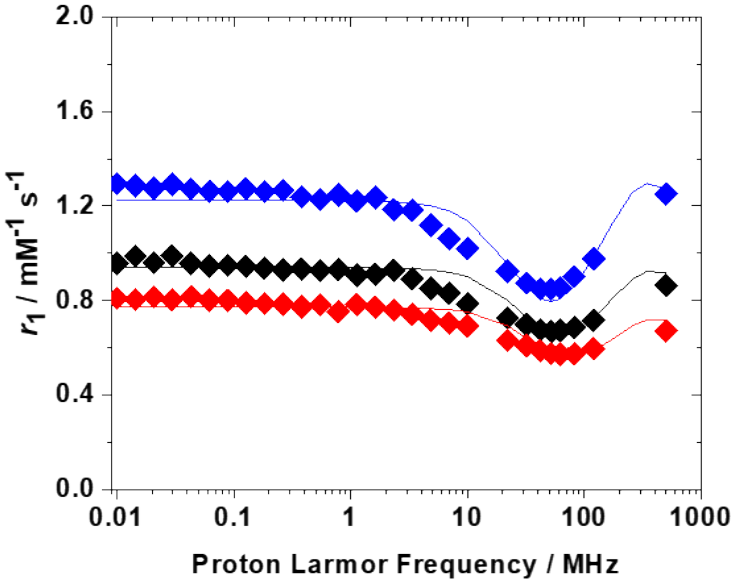

Figure S19. ^{1}H NMRD profiles of [Fe(DETA)] in aqueous solution at pH = 4.3 and at different temperatures (10°C, blue; 25°C, black; 37°C, red); [Fe^{3+}] = 3.2 mM.

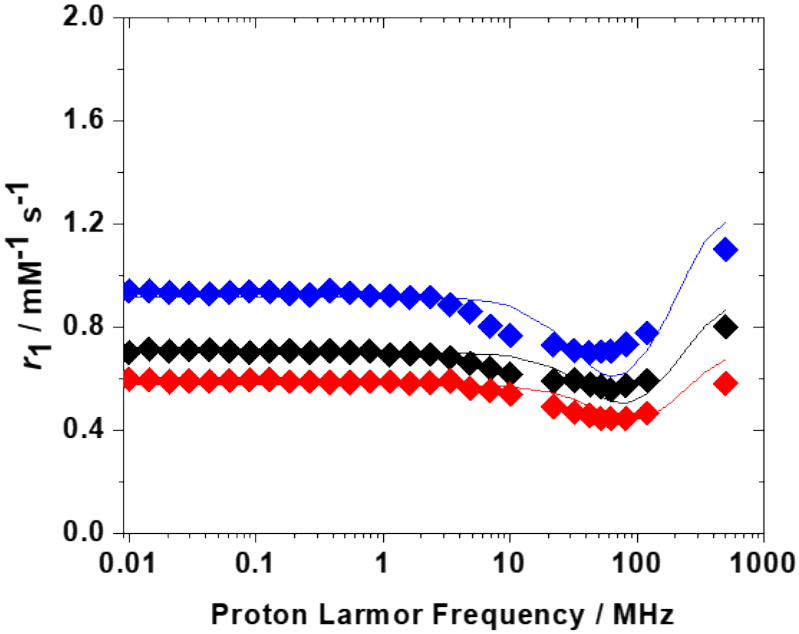

Figure S20. ^{1}H NMRD profiles of [Fe(UNTA)] in aqueous solution at pH = 7 and at different temperatures (10°C, blue; 25°C, black; 37°C, red); [Fe^{3+}] = 3.8 mM.

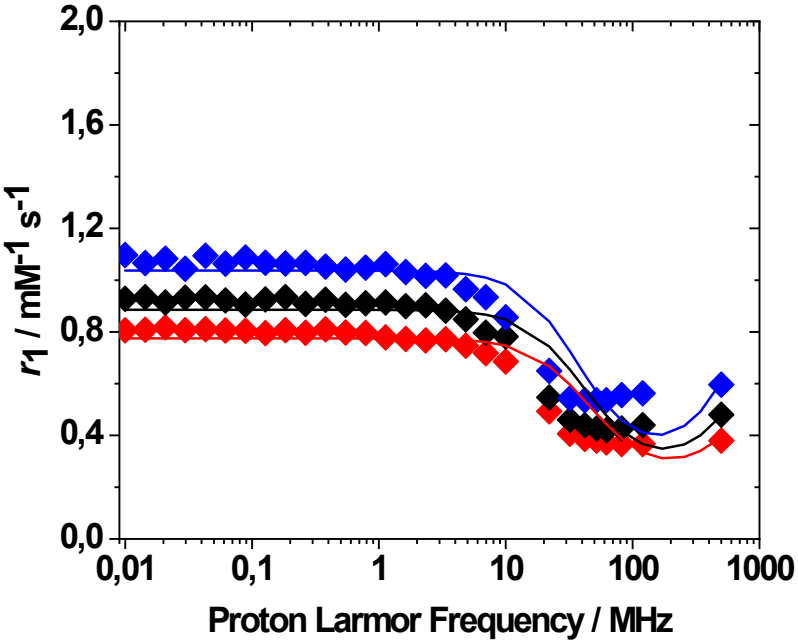

Figure S21. ^{1}H NMRD profiles of [Fe(DOTRA)] in aqueous solution at pH = 7 and at different temperatures (10°C, blue; 25°C, black; 37°C, red); [Fe^{3+}] = 1.5 mM.

VII. References

1) J. L. Sudmeier and C. N. Reilley, *Anal. Chem.*, **1964**, *36*, 1698

2) C. F. G. C. Geraldes, A. D. Sherry, M. P. M. Marques, M. C. Alpoim, S. Cortes, *J. Chem. Soc. Perkin Trans. 2*, 1991, 137 – 146

3) R. L. Gustafson, A. E. Martell, *J. Phys. Chem.* **1963**, *67*, 576–582.

4) R. Ma, R. Motekaitis, A. Martell, *Inorg. Chim. Acta.*, **1994**, *224*, 151.

5) Gaussian 16, Revision C.01, Frisch, M. J.; Trucks, G. W.; Schlegel, H. B.; Scuseria, G. E.; Robb, M. A.; Cheeseman, J. R.; Scalmani, G.; Barone, V.; Petersson, G. A.; Nakatsuji, H.; Li, X.; Caricato, M.; Marenich, A. V.; Bloino, J.; Janesko, B. G.; Gomperts, R.; Mennucci, B.; Hratchian, H. P.; Ortiz, J. V.; Izmaylov, A. F.; Sonnenberg, J. L.; Williams-Young, D.; Ding, F.; Lipparini, F.; Egidi, F.; Goings, J.; Peng, B.;Petrone, A.; Henderson, T.; Ranasinghe, D.; Zakrzewski, V. G.; Gao, J.; Rega, N.; Zheng, G.; Liang, W.; Hada, M.; Ehara, M.; Toyota, K.; Fukuda, R.; Hasegawa, J.; Ishida, M.; Nakajima, T.; Honda, Y.; Kitao, O.; Nakai, H.; Vreven, T.; Throssell, K.; Montgomery, J. A., Jr.; Peralta, J. E.; Ogliaro, F.; Bearpark, M. J.; Heyd, J. J.; Brothers, E. N.; Kudin, K. N.; Staroverov, V. N.; th, T. A.; Kobayashi, R.; Normand, J.;Raghavachari, K.; Rendell, A. P.; Burant, J. C.; Iyengar, S. S.; Tomasi, J.; Cossi, M.; Millam, J. M.; Klene, M.; Adamo, C.; Cammi, R.; Ochterski, J. W.; Martin, R. L.; Morokuma K.; Farkas, O.; Foresman, J . B.; Fox, D. J. Gaussian, Inc., Wallingford CT, **2016**.

6) Becke, A. D. *J. Chem. Phys.* **1993**, 98, 5648– 5652.

7) Jensen, F. *J. Chem. Theory Comput*. **2014**, 10, 1074– 1085.

8) Lu, T.; Chen, Q. *Chem.: Methods* **2021**, 1, 231– 239.

9) Bader, R. F. W. *Chem. Rev*. **1991**, 91, 893– 928.

10) AIMAll (Version 11.05.16), Todd A. Keith, TK Gristmill Software, Overland Park KS, USA, **2011** (aim.tkgristmill.com).

11) Lu, T.; Chen, F. *J. Comput. Chem*. **2012**, 33, 580– 592.

12) Humphrey, W.; Dalke, A.; Schulten, K., *J. Molec. Graphics*, **1996**, 14, 33-38.